Asian Journal of Atmospheric Environment

TECHNICAL INFORMATION Open Access

Natural cleaning effects on deposited atmospheric particles: a case study of Asian dust, pollen, and volcanic ash

Kenji Miki[1*]

Abstract
Natural atmospheric particles, such as yellow sand, pollen, and volcanic ash, are frequently deposited on exposed surfaces, potentially reducing the optical performance of solar panels and other transparent systems. However, the removability of these particle types under environmental conditions has not been compared systematically. In this work, we conducted laboratory experiments to evaluate the removability of yellow sand, pollen, and volcanic ash deposited on slide glass surfaces as representative natural particulates. Controlled wind and simulated rainfall were applied separately and in combination to investigate particle adhesion and cleaning behavior. Although pollen was efficiently removed by wind, it had the greatest effect on light transmittance per unit weight. In contrast, yellow sand exhibited strong adhesion and low removability.

Keywords PV panel, Yellow sand, Pollen, Ash, Soiling effect

1 Introduction

Although solar energy is a leading candidate for sustainable energy production, the soiling effect caused by airborne particles deposited on photovoltaic (PV) panels strongly affects the energy production efficiency of PV panels (Bergin et al., 2017; Hasan et al., 2021; Khalid et al., 2023). The pollutants deposited on PV panels include mineral dust, pollen, fungal spores, engine exhaust gas, and agricultural emissions (Nezamisavojbolaghi et al., 2023). The soiling effect is strong enough to negate the improvements in PV efficiency in Asia and the Middle East (Ilse et al., 2019). Previous studies have addressed countermeasures against the soiling effects of airborne particle deposition (Abd-Elhady et al., 2024; Adekanbi et al., 2024), and their results have been applied to the maintenance of PV panels in desert areas (Cordero et al., 2018), tropical regions (Andrea et al., 2019), and urban areas with chimneys (Radonjić et al., 2021). Coating technologies (Syafiq et al., 2022), washing systems for PV panels using rainwater (Myyas et al., 2022), and automated cleaning devices for PV panels (Kazem, 2023) have been developed.

The natural removal effects of rain and wind have also been studied (Ramírez-Revilla et al., 2022). For example, a previous study suggested that when wind and rain are strong enough, the soiling effect on PV panels is weakened (Stankov and Terziev, 2024). Furthermore, when a high density of particles is deposited on PV panels, the removal effect on the particles increases (Yao et al., 2023). Simulation results suggest that larger particles (100–500 μm) are more effectively removed by the removal effect of wind (Han et al., 2026).

The soiling effect also depends on the particle types. For example, among ash, soil, cement, brick dust, wood

*Correspondence:
Kenji Miki
miki39865@criepi.denken.or.jp
[1]Central Research Institute of Electric Power Industry, 1646 Abiko, Abiko-shi, Chiba 2701194, Japan

dust, sand, and sea salt, the soiling effect of wood dust is the greatest (Lenko et al., 2024). Regarding the washing effect, when pollen grains are soaked in water, small protein particles called the Ubisch bodies detach from the grains and remain on PV panels, which decreases the transmittance in the UV wavelength range (Miki & Mori, 2025). Observations in various regions have reported that soiling effects are stronger in the UV wavelength range than other wavelengths (Smestad et al., 2020). However, there has been limited research on the natural removal processes that affect various types of particles.

In this study, the types of airborne dust with the greatest effect in East Asian regions, Asian dust (yellow sand) (e.g., Hagiwara et al., 2020), pollen (e.g., Miki & Mori, 2025), and volcanic ash (Nishioka & Ota, 2015), were deposited on slides (25 mm × 75 mm), and the removal effects of wind and rain were experimentally analyzed. Yellow sand storms are known to have a serious impact on PV panel performance, and the use of protective walls was proposed in a previous study conducted in China (Pui et al., 2014). Concerning pollen, it has been reported that the degradation of PV panel efficiency caused by pollen deposition can be significant and may not be recoverable even after rainfall (Bessa et al., 2024). Ashfall tephra can cause large-scale shutdown of PV panels (Zorn & Walter, 2016). This study aimed to clarify the removal characteristics of each particle type and support the development of region-specific PV panel maintenance methods that consider local airborne particle properties and meteorological conditions.

2 Materials and methods

Samples of yellow sand (Mono Planning Ltd., Saitama, Japan), pollen (*Cryptomeria japonica*) (Yamizo Kafun Kenkyukai, Ibaraki, Japan), and volcanic ash particles (Kenis Ltd. Osaka, Japan) were dispersed on glass slides, which were then gently turned upside down and back to settle the particles (Fig. 1 (left)). The slides were placed on an inclined plane (KKS-90 4–6519-02, Asone, Japan) with a 15° slope (Fig. 1 (right)), which was determined to be the optimum angle for solar panels (Pascal & Ganapathisubbu, 2011; Solyali & Mollaei, 2025), and exposed to controlled wind and simulated rain.

The initial state of the slides without dispersed particles is referred to as "α" and the state after the particle dispersion and settling procedure is referred to as "β". The state after exposure to wind is referred to as "γ_w", and the state after exposure to simulated rain is referred to as "γ_r". For each state, the transmittance at visible (380–760 nm), UV (365 nm), and IR (940 nm) wavelengths was measured five times at randomly selected locations on the slides using a transmission meter (LS162, Shenzhen Linshang Technology Co., Ltd., China). The cleaning effects of wind and rain were evaluated based on Lambert–Beer law, which is expressed as

$$\ln\left(\frac{I_\beta}{I_\gamma}\right) = -a_1 c_1 \Delta L \tag{1}$$

$$\ln\left(\frac{I_\gamma}{I_\alpha}\right) = -a_2 c_2 \Delta L, \tag{2}$$

where a_1 (g^{-1} cm^2) and a_2 (g^{-1} cm^2) are the coefficients, I_α is the transmitted light intensity in state α, I_β is the transmitted light intensity in state β, I_γ is the transmitted light intensity in state γ, c (g cm^{-3}) is the concentration of accumulated particles, L (cm) is the optical path length. Based on eqs. (1)-(2), the logarithm of the transmittance ratio is proportional to ΔL. Thus, I_α, I_β, and I_γ were observed and $\ln\left(\frac{I_\beta}{I_\gamma}\right)$ and $\ln\left(\frac{I_\gamma}{I_\alpha}\right)$ were calculated as indices of relative amount of accumulated particles.

For the evaluation, the five measurements for each state were averaged by

$$-\ln\left(\frac{I_\alpha}{I_\beta}\right) = -\frac{1}{5}\sum_{i=1}^{5}\ln\left(\frac{I_{\alpha i}}{I_{\beta_i}}\right) \tag{3}$$

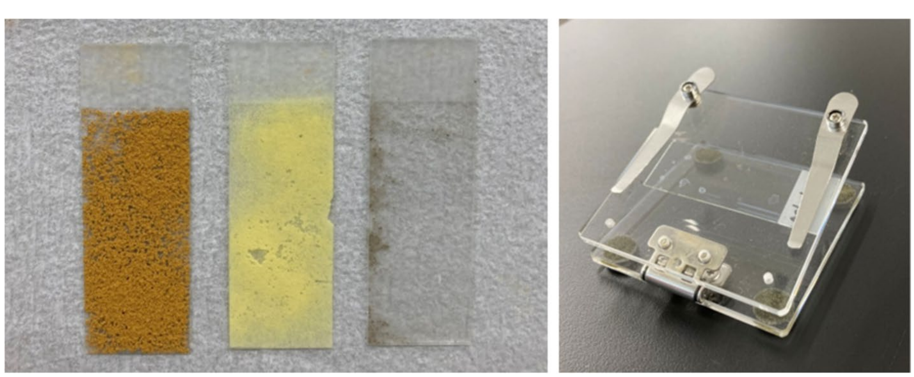

Fig. 1 (Left) Slides with deposited yellow sand, pollen, and volcanic ash. (Right) Slide placed on an inclined plane

Table 1 Particle weight for each particle type at each state in the wind removal experiment

Y. sand			
	Test 1	Test 2	Test 3
m_α (g)	4.919	4.924	4.925
m_β (g)	4.981	4.971	5.000
m_{yw} (g)	4.971	4.956	4.998
m_β-m_α (g)	0.062	0.047	0.075
m_{yw}-m_α (g)	0.052	0.032	0.073
(m_{yw}-m_α)/(m_β-m_α)	0.839	0.681	0.973
Pollen			
	Test 1	**Test 2**	**Test 3**
m_α (g)	4.936	4.927	4.931
m_β (g)	4.991	4.961	5.005
m_{yw} (g)	4.956	4.942	4.952
m_β-m_α (g)	0.055	0.034	0.074
m_{yw}-m_α (g)	0.020	0.015	0.021
(m_{yw}-m_α)/(m_β-m_α)	0.364	0.441	0.284
Ash			
	Test 1	**Test 2**	**Test 3**
m_α (g)	4.933	4.926	4.933
m_β (g)	4.941	4.930	4.937
m_{yw} (g)	4.936	4.93	4.934
m_β-m_α (g)	0.008	0.004	0.004
m_{yw}-m_α (g)	0.003	0.004	0.001
(m_{yw}-m_α)/(m_β-m_α)	0.375	1.000	0.250

Generally, when x and y are variables, the standard errors were calculated using the error propagation formula, which is expressed as

$$Var\left[f\left(x+\Delta x, y+\Delta y\right)\right] \approx \left(\frac{\partial f}{\partial x}\right)^2 (\Delta x)^2 + \left(\frac{\partial f}{\partial y}\right)^2 (\Delta y)^2 \quad (4)$$

Thus, by substituting the measurement results into Eq. (4), average variance $-\ln\left(\frac{I_\alpha}{I_\beta}\right)$ is derived by

$$Var\left[-\ln\left(\frac{I_\alpha}{I_\beta}\right)\right] \approx \left(\frac{\Delta I_\alpha}{I_\alpha}\right)^2 + \left(\frac{\Delta I_\beta}{I_\beta}\right)^2 \quad (5)$$

where ΔI is the error of each result. Thus, the average standard error is given as

$$\sigma_{\ln\left(\frac{I_\alpha}{I_\beta}\right)} = \sqrt{\left(\frac{\Delta I_\alpha}{I_\alpha}\right)^2 + \left(\frac{\Delta I_\beta}{I_\beta}\right)^2}, \quad (6)$$

2.1 Cleaning effect of wind

In the experimental setup, controlled wind was generated using a blower (B0BTPG97V8, Shenzhen Gdstime Technology Co., Ltd., China) and delivered to the wind exposure area through a cardboard wind tunnel (6 cm high, 6 cm wide, and 90 cm long). The slides with dispersed particles were placed at the outlet of the wind tunnel in the wind exposure area and exposed to controlled wind at 5 m s^{-1} for 1 min. The experiment was performed three times (Test 1–3) and the transmittance at each state was measured.

Table 2 Particle weight for each particle type at each state in the rain removal experiment

Y. sand			
	Test 1	**Test 2**	**Test 3**
m_α (g)	4.910	4.930	4.925
m_β (g)	4.975	4.979	5.046
m_{yr} (g)	4.936	4.927	4.931
m_β-m_α (g)	0.065	0.049	0.121
m_{yr}-m_α (g)	0.026	−0.003	0.006
(m_{yr}-m_α)/(m_β-m_α)	0.400	−0.061	0.050
Pollen			
	Test 1	**Test 2**	**Test 3**
m_α (g)	4.935	4.927	4.931
m_β (g)	5.022	4.994	4.991
m_{yr} (g)	4.936	4.927	4.931
m_β-m_α (g)	0.087	0.067	0.060
m_{yr}-m_α (g)	0.001	0.000	0.000
(m_{yr}-m_α)/(m_β-m_α)	0.011	0.000	0.000
Ash			
	Test 1	**Test 2**	**Test 3**
m_α (g)	4.935	4.926	4.932
m_β (g)	4.941	4.927	4.936
m_{yr} (g)	4.935	4.926	4.933
m_β-m_α (g)	0.006	0.001	0.004
m_{yr}-m_α (g)	0.000	0.000	0.001
(m_{yr}-m_α)/(m_β-m_α)	0.000	0.000	0.250

2.2 Cleaning effect of rain

The slides with particles were placed on the target plate area and simulated rain was sprayed with a water sprinkler (Iris Oyama, Tokyo, Japan) for 1 min from a height of 60 cm and distance of 80 cm at a spray rate of 276 mm h^{-1}, which was the minimum available spray rate of the sprinkler. The slides were then covered with aluminum foil and dried at room temperature. The experiment was performed three times (Test 1–3) and the transmittance at each state was measured.

3 Results

Yellow sand, followed by pollen, showed the highest weight of particles settled on the slide (Tables 1 and 2). Pollen, followed by volcanic ash, showed the highest ratio of weight washed out by the wind. Pollen, followed by yellow sand, showed the highest weight of particles washed out by wind (Table 1). The relationship between the weight of particles removed by the wind and the changes in the transmitted light intensities indicated that these two factors are highly related, regardless of the particle type ($r^2 = 0.87, p < 0.01$) (Fig. 2a). No clear wavelength dependence was observed in the overall relationship. The changes in the transmitted light intensities and the weight of particles that remained after the exposure to wind also showed a clear relationship regardless of the particle type ($r^2 = 0.58, p < 0.01$) (Fig. 2b).

In contrast, almost all the particles deposited on the slide were washed out by the simulated rain. However, the results show that yellow sand was more likely to remain after the removal (Table 2). The relationship between the weight of particles washed out by the simulated rain and the changes in the transmitted light intensities showed that when a similar weight was washed out, pollen showed larger changes in transmittance than yellow sand (Fig. 3a). Almost all particles were washed out by the simulated rain; thus, the weights of particles remaining after the removal were within the experimental error (Fig. 3b). After the removal, the effect on the wavelength in the visible and the UV wavelength range remained greater than that on the IR wavelength range.

$$R = \begin{cases} \frac{1}{600}\lambda - 0.5(300nm \leq \lambda < 900nm) \\ -\frac{1}{300}\lambda + 4(900nm \leq \lambda < 1200nm) \\ 0(\lambda < 300nm, 1200nm \leq \lambda) \end{cases} \quad (7)$$

By assuming that the transmittances in the wavelength range of visible, UV, and IR are uniform, the theoretical influence of the particle removal on power generation efficiencies in this experiment was calculated. An ideal spectral response was used in the calculation (Raju Anand et al., 2012). The spectral response (R) in each wavelength range is calculated as:

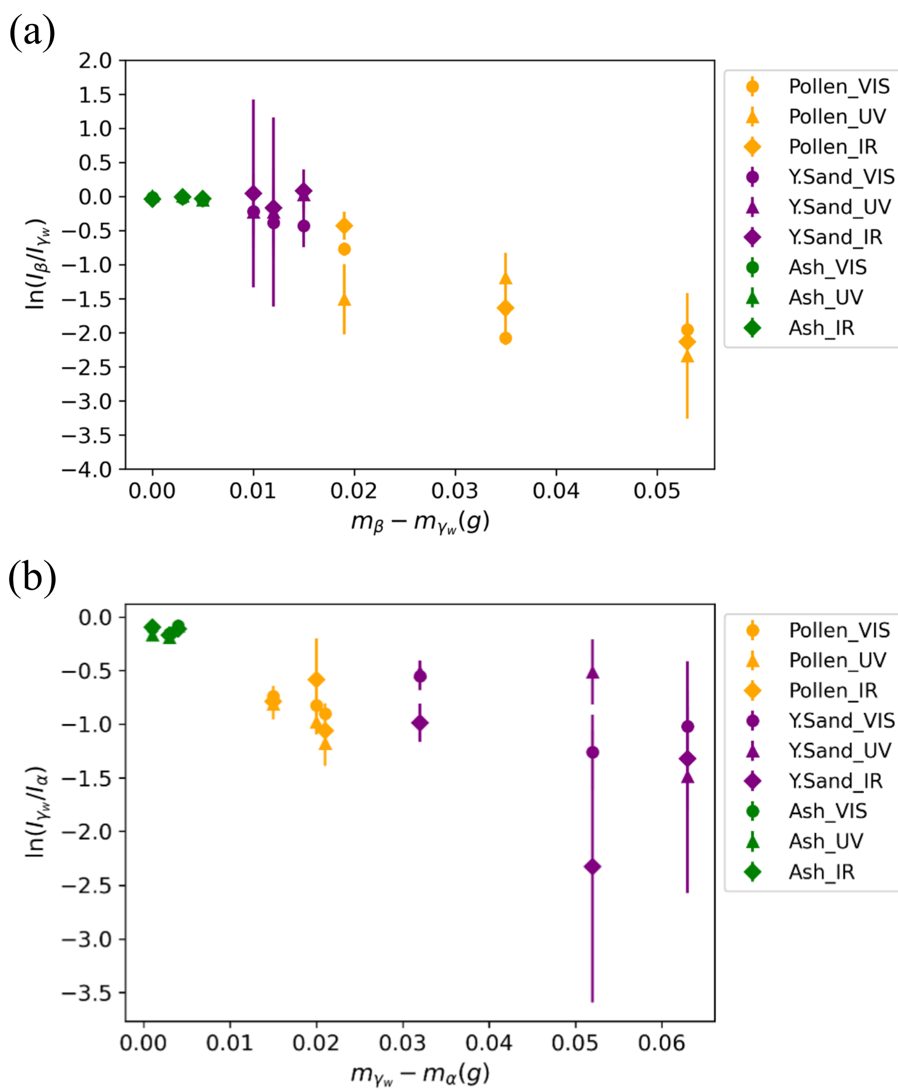

Fig. 2 Relationship between the change in deposited particle weight and the transmittance ratio between (**a**) β and γ, and (**b**) α and γ in the wind removal effect experiment

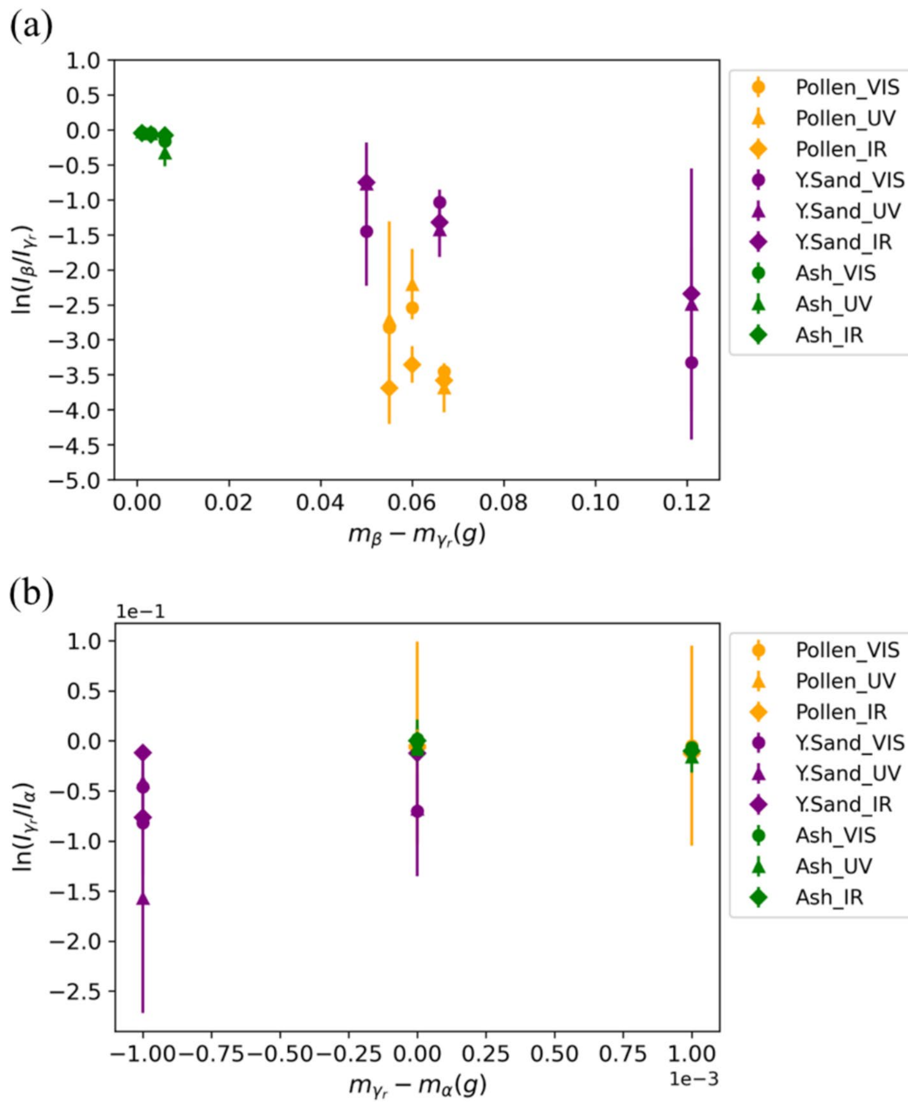

Fig. 3 Relationship between the change in deposited particle weight and the transmittance ratio between (**a**) β and γ, and (**b**) α and γ in the simulated rain removal effect experiment

When E_β and E_γ are the power generation efficiencies of state β and γ, respectively,

$$E_{\beta,\gamma} = \int_{300}^{1200} \frac{I_{\beta,\gamma}(\lambda)}{I_0(\lambda)} R(\lambda)\,\mathrm{d}\lambda \approx \frac{\sum_{\lambda=300}^{1199} \frac{I_{\beta,\gamma}(\lambda)}{I_0(\lambda)} R(\lambda)\,\Delta\lambda + \sum_{\lambda=301}^{1200} \frac{I_{\beta,\gamma}(\lambda)}{I_0(\lambda)} R(\lambda)\,\Delta\lambda}{2} \quad (8)$$

where I_0 is the incident light intensity and $\Delta\lambda = 1(\mathrm{nm})$ was substituted in the calculation.

The influence of the removal effect on the power generation efficiency was evaluated using E_{ratio} as follows:

$$E_{ratio} = \frac{E_\gamma}{E_\beta} \quad (9)$$

The E_{ratio} values for yellow sand, pollen, and ash for the removal of the controlled wind were 1.16, 5.37, and 1.02, respectively (Fig. 4). On the other hand, the E_{ratio} values for yellow for the removal of the controlled rain were 4.77, 17.58, and 1.15, respectively (Fig. 5).

4 Discussion

In both the controlled wind and simulated rain experiments, only a limited weight of volcanic ash settled on the slide, resulting in unclear changes in transmittance. However, even when changes in the weight of the settled volcanic ash were observed, no corresponding changes in transmittance were detected, regardless of the wavelength range (Fig. 2a).

In wind-induced removal, yellow sand showed only limited recovery of transmittance especially in the infrared regions, whereas relatively large recovery was observed in the visible region (Fig. 4). This result suggests that the wind treatment may have caused size-dependent

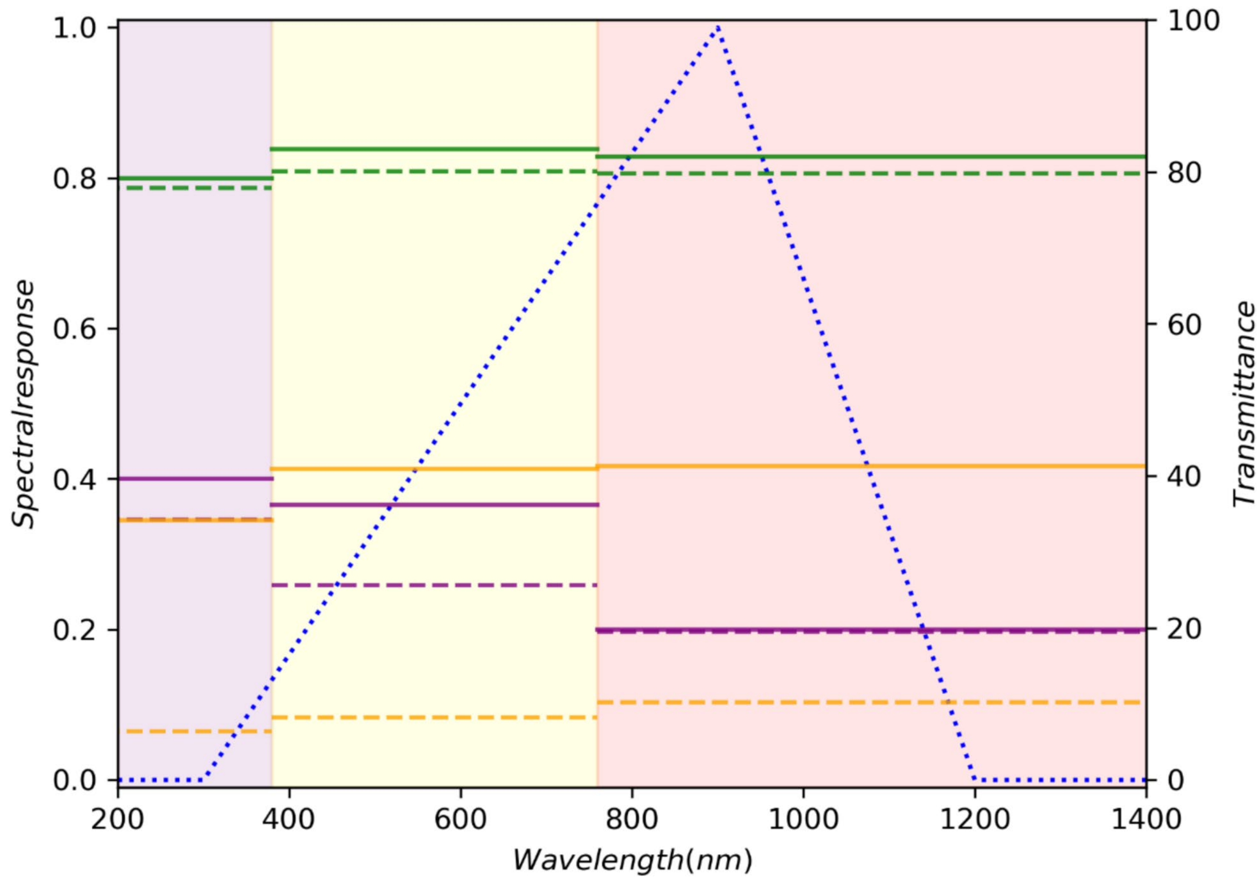

Fig. 4 Ideal spectral response (blue dotted line) and transmittance of pollen (yellow), yellow sand (purple), and ash (green) across UV, visible, and IR wavelengths, before (dashed lines) and after (solid lines) wind-induced particle removal

selective removal. For idealized particles, the threshold friction velocity has been shown to reach a minimum at intermediate particle sizes and to increase toward smaller sizes because of interparticle cohesion and toward larger sizes because of gravity (Shao & Lu, 2000). In addition, yellow sand particles have been reported to occur as aggregates (Jeong, 2008), suggesting that relatively small particles and relatively large particles may have remained in the present study as well. However, particle-size selectivity alone cannot fully explain the wavelength-dependent differences in transmittance recovery, and spatial heterogeneity and differences in the aggregation state of the residual particles may also have contributed.

When pollen grains were removed by simulated rain, no effect on the UV wavelength range caused by the Ubisch bodies, as reported in a previous study, was observed (Miki & Mori, 2025). For the same weight, pollen grains had a greater effect on transmittance than yellow sand (Fig. 2a). However, yellow sand tended to remain on the slides after the removal. The weight of particles after settling on the slide and removal by wind and rain reflects the adhesion properties of each particle type.

The physical adhesion properties of particles have been studied in previous studies (Baraka et al., 2024; Huang et al., 2022; Liu et al., 2021; Zhao et al., 2021). In the simplified adhesion model (Ibrahim et al., 2003), the condition under which a particle is lifted directly by turbulence is

$$F_L > F_{adh} + mg \tag{10}$$

where F_L is the lift force, F_{adh} is the adhesion force, m is the particle mass, and g is gravitational acceleration. F_{adh} includes the van der Waals force (F_{VDW}), electrostatic force (F_{Elec}) (Dahham et al., 2023), and liquid film force (F_{Liq}) (Hinds, 1999). Van der Waals force is generally calculated as

$$F_{VDW} = \frac{A_H d}{12D^2} \tag{11}$$

where A_H is the Hamaker constant, D is the distance between the surface and a particle or particles, and d is the diameter of a particle. The electrostatic force is calculated as

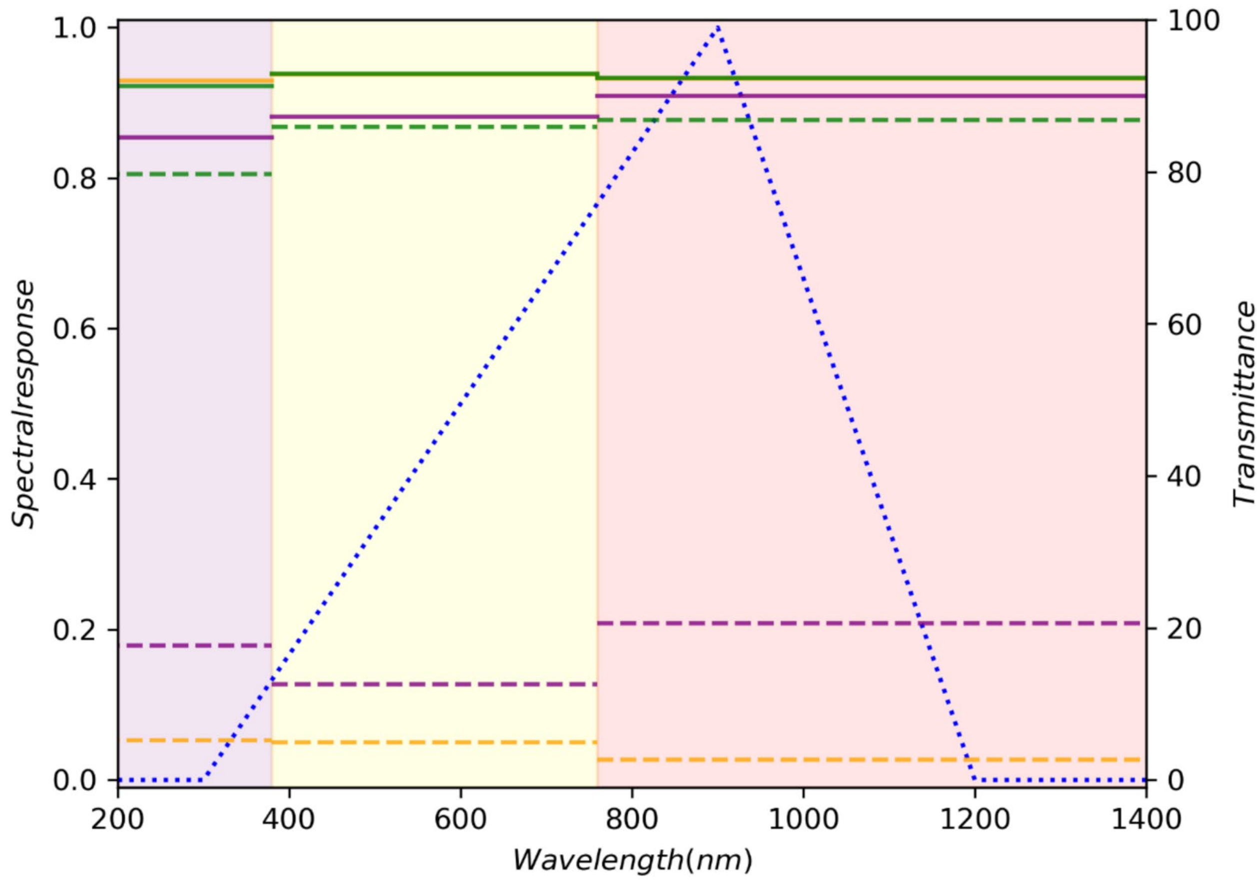

Fig. 5 Ideal spectral response (blue dotted line) and transmittance of pollen (yellow), yellow sand (purple), and ash (green) across UV, visible, and IR wavelengths, before (dashed lines) and after (solid lines) rain-induced particle removal

$$F_{Elec} = \frac{K_E q^2}{D_q^2} \tag{12}$$

where K_E is a constant of proportionality, q is the electric charge of a particle, and D_q is the separation distance of opposite charges. Because the equilibrium charge is proportional to $d^{\frac{1}{2}}$ (Hinds, 1999),

$$F_{Elec} = \frac{K_E k d}{D_q^2} \tag{13}$$

where k is a constant.

The liquid film force is empirically calculated (Hinds, 1999) as

$$F_{Liq} = C_{Liq} d \tag{14}$$

where RH is relative humidity (%). Here, C_{Liq} is a coefficient derived as

$$C_{Liq} = 6.3 \times 10^{-2} \left(1 + 0.009\,(RH)\right) \tag{15}$$

Drag force (F_D) on a particle from ambient flow is given as

$$F_D = \frac{C_D \pi d^2 v^2 \rho}{8} \tag{16}$$

where C_D is the drag coefficient, v is the wind speed, and ρ is the particle density. Thus, when the drag force is equal to the lift force, the ratio of the lift force to adhesion force on a particle is

$$\frac{F_D}{F_{VDW} + F_{Elec} + F_{Liq}} = \frac{\frac{C_D \pi d^2 v^2 \rho}{8}}{\frac{A_H d}{12D^2} + \frac{K_E k d}{D_q^2} + C_{Liq} d} = \frac{C_D \pi v^2 \rho d^2}{8d\left(\frac{A_H}{12D^2} + \frac{K_E k}{D_q^2} + C_{Liq}\right)} \propto d, \tag{17}$$

According to previous studies, yellow sand has the finest particles (diameter: 4 μm) (Mori et al., 2003), compared with *C. japonica* pollen (diameter: 30 μm) (Miki et al., 2021) and volcanic ash (diameter: ~ 100 μm) (Poulidis et

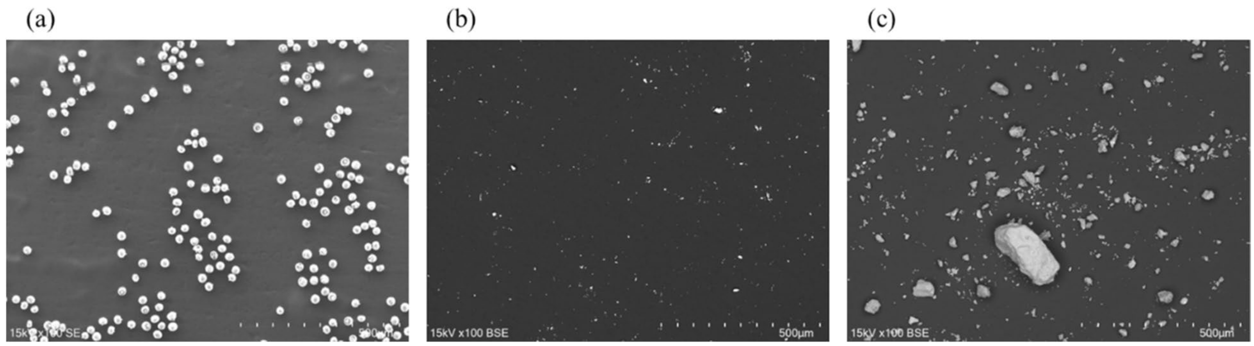

Fig. 6 SEM images of (**a**) pollen (**b**) yellow sand, and (**c**) ash

al., 2017). Scanning Electron Microscope (SEM) images were also obtained using TM 4000Plus (Hitachi, Tokyo, Japan) (Fig. 6), and the Feret diameters of each sample were analyzed using Fiji (Schindelin et al., 2012). The analysis showed that the mean Feret diameters of yellow sand and pollen were 3.6 ± 2.3 μm and 38.1 ± 17.9 μm, respectively, which is consistent with the previous studies. Thus, it is reasonable that yellow sand remained on the slide most efficiently after removal by wind and simulated rain. For ash, the image analysis showed a mean Feret diameter of 6.4 ± 5.9 μm and a maximum Feret diameter of 83.1 μm, which was also consistent with the previous study. The amount of ash deposited on the slide was small, and the transmittance change remained unclear. Therefore, the present experiment was not sufficient to evaluate the removability of ash with the same robustness as for yellow sand or pollen.

Hence, differences in the removal and adhesion properties of yellow sand, pollen, and volcanic ash were experimentally observed. The results suggest that although the effect of wavelength is limited, small fragments from yellow sand or pollen grains may persist for a long time after removal because of their strong adhesion. It has also been reported that other environmental conditions, such as humidity and the combined effects of wind and rain, can influence the adhesion of particles on PV panels (Styszko et al., 2019). Thus, more complex environmental conditions need to be examined to analyze actual particle removal under realistic field conditions.

5 Conclusion

This study experimentally compared the removability of yellow sand, pollen, and volcanic ash deposited on glass slides under controlled wind and simulated rain conditions. Each particle type exhibited distinct adhesion and removal characteristics. Pollen was easily removed by wind but substantially reduced light transmittance per unit mass, whereas yellow sand adhered strongly and resisted removal. In contrast, the volcanic ash used in this study did not settle on the slides as efficiently as yellow sand or pollen did. These findings may contribute to improving cleaning systems for PV panels and increasing the PV efficiency in regions with high concentrations of airborne particles.

Acknowledgements
Not applicable.

Authors' contributions
Draft writing, material preparation, data collection and analysis, were performed by Kenji Miki.

Funding
Not applicable.

Data availability
The authors confirm that the data supporting the findings of this study are available within the article. The code that was used for this experiment was established following the equations.

Declarations

Ethics approval and consent to participate
Not applicable.

Competing interests
The authors declare no competing interests.

Received: 8 January 2026 / Accepted: 3 April 2026
Published online: 22 April 2026

References

Abd-Elhady, M. S., Rana, A., Elsebaaie, M. A., & Kandil, H. A. (2024). A new cleaning method for solar panels inspired from the natural vibrations of tree branches and leaves. *Scientific Reports, 14*, 18138.

Adekanbi, M. L., Alaba, E. S., John, T. J., Tundealao, T. D., & Banji, T. I. (2024). Soiling loss in solar systems: A review of its effect on solar energy efficiency and mitigation techniques. *Cleaner Energy Systems, 7*, 100094.

Andrea, Y., Pogrebnaya, T., Kichonge, B. (2019). Effect of industrial dust deposition on photovoltaic module performance: experimental measurements in the tropical region. *International Journal of Photoenergy*, *2019*, 1892148.

Baraka, A. E., En-nadir, R., Kabatas, M.A.B.-M., & Khaldoun, A. (2024). Soiling, adhension, and surface characterization of concentrated solar power reflectors: Insights and challenges in the MENA region. *Sustainability, 16*, 6257.

Bergin, M. H., Ghoroi, C., Dixit, D., Scahuer, J. J., & Shindell, D. T. (2017). Large reduction in solar energy production due to dust and particulate air pollution. *Environmental Science & Technology Letters, 4*, 339–344.

Bessa, J. G., Valerino, M., Muller, M., Bergin, M., Micheli, L., & Almonacid, F. (2024). An investigation on the pollen-induced soiling losses in utility-scale PV plants. *IEEE Journal of Photovoltaics, 14*, 178–184.

Cordero, R. R., Damiani, A., Laroze, D., MacDonell, S., Jorquera, J., Sepúlveda, E., Feron, S., Llanillo, P., Labbe, F., Carrasco, J., Ferrer, J., & Torres, G. (2018). Effects of soiling on photovoltaic (PV) modules in the Atacama Desert. *Scientific Reports, 8*, 13943.

Dahham, I. A., Zainuri, M. A. A. M., Abdullah, A. A., & Fauzan, M. F. (2023). Modeling the effect of dust and wind speed on solar panel performance in Iraq. *Energies, 16*, 6397.

Hagiwara, K., Matsumoto, T., Tsedendamba, P., Baba, K., & Hoshino, B. (2020). Distribution of viable bacterial in the dust-generating natural source area of the Gobi region, Mongolia. *Atmosphere, 11*, 893.

Han, Z., Lu, H., Zhao, W., & Zheng, C. (2026). Sand particle deposition and re-suspension characteristics of PV modules and the effects on PV efficiency: Based on CFD-DEM simulation. *Renewable Energy, 256*, 123817.

Hasan, K., Yousuf, S. B., Tushar, M. S. H. K., Das, B. K., Das, P., & Islam, M. S. (2021). Effects of different environmental and operational factors on the PV performance: A comprehensive review. *Energy Science & Engineering, 10*, 656–675.

Hinds, W. C. (1999). *Aerosol technology: Properties, behaviour, and measurement of airborne particles*, 2nd ed. John Wiley & Sons.: NJ, United States, 1999; pp. 142–144.

Huang, P., Hu, G., Zhao, X., Lu, L., Ding, H., & Li, J. (2022). Effect of organics on the adhesion of dust to PV panel surfaces under condensation. *Energy, 261*, 125255.

Ibrahim, A. H., Dunn, P. F., & Brach, R. M. (2003). Microparticle detachment from surfaces exposed to turbulent air flow: Controlled experiments and modeling. *Journal of Aerosol Science, 34*, 765–782.

Ilse, K., Micheli, L., Figgis, B. W., Lange, K., Daßler, D., Hanifi, H., Wolfertstetter, F., Naumann, V., Hagendorf, C., Gottschalg, R., & Bagdahn, J. (2019). Techno-economic assessment of soiling losses and mitigation strategies for solar power generation. *Joule, 3*, 2303–2321.

Jeong, G. Y. (2008). Bulk and single-particle mineralogy of Asian dust and a comparison with its source soils. *Journal of Geophysical Research, 113*, D02208.

Kazem, H. A. (2023). Dust impact on the performance of solar photovoltaic module: A new prospect. *Energy Sources, Part a: Recovery, Utilization, and Environmental Effects, 45*, 4087–4106.

Khalid, H. M., Rafique, Z., Muyeen, S. M., Raqeeb, A., Said, Z., Saidur, R., & Sopian, K. (2023). Dust accumulation and aggregation on PV panels: An integrated survey on impacts, mathematical models, cleaning mechanisms, and possible sustainable solution. *Solar Energy, 251*, 261–285.

Lenko, S. R., Goel, S., Satpathy, P. R., Goel, S., Satpathy, P. R., Jena, B., & Sharma, R. (2024). Investigation of performance reduction of PV system due to environmental dust: Indoor and real-time analysis. *E-Prime - Advances in Electrical Engineering, Electronics and Energy, 9*, 100657.

Liu, X., Yue, S., Lu, L., & Li, J. (2021). Settlement-adhesion evolution mechanism of dust particles in the flow field of photovoltaic mirrors at night. *Chemical Engineering Research & Design, 168*, 146–155.

Miki, K., & Mori, S. (2025). Seasonal variation in photovoltaic generation efficiency due to bioaerosol particle accumulation. *Sustainable Energy Technologies and Assessments, 73*, 104106.

Miki, K., Fujita, T., & Sahashi, N. (2021). Development and application of a method to classify airborne pollen taxa concentration using light scattering data. *Scientific Reports, 11*, 22371.

Mori, I., Nishikawa, M., Tanimura, T., & Quan, H. (2003). Change in size distribution and chemical composition of kosa (Asian dust) aerosol during long-range transport. *Atmospheric Environment, 37*, 4253–4263.

Myyas, R. N., Al-Dabbasa, M., Tostado-Véliz, M., & Jurado, F. (2022). A novel solar panel cleaning mechanism to improve performance and harvesting rainwater. *Solar Energy, 237*, 19–28.

Nezamisavojbolaghi, M., Davodian, E., Bouich, A., Tlemçani, M., Mesbahi, O., & Janeiro, F. M. (2023). The impact of dust deposition on PV panels' efficiency and mitigation solutions: Review article. *Energies, 16*, 8022.

Nishioka, K., & Ota, Y. (2015). Impact of volcanic ash on output of photovoltaic systems. *Journal of the Institute of Electrical Engineers of Japan, 35*, 348–353. (in Japanese).

Pascal, F., & Ganapathisubbu, S. (2011). Tracking benefits for solar collectors installed in Bangalore. *Journal of Renewable and Sustainable Energy, 3*, 023103.

Poulidis, A. P., Takemi, T., Iguchi, M., & Renfrew, I. A. (2017). Orographic effects on the transport and deposition of volcanic ash: A case study of mount Sakurajima, Japan. *JGR Atmospheres, 122*, 9332–9350.

Pui, D. Y. H., Cao, J., An, Z., & Wang, J. (2014). Great wall of solar panels to mitigate yellow dust storm. *Particuology, 13*, 146–150.

Radonjić, I., Pavolvić, T., Mirjanić, D., & Pantić, L. (2021). Investigation of fly ash soiling effects on solar modules performances. *Solar Energy, 220*, 144–151.

Raju Anand, Y., Vijay Kumar, R., & Rudramoorthy, R. (2012). Thermal efficiency improvement of solar PV module by spectral absorption using water. 2012 International Conference on Power and Energy Systems (ICPES 2012) IPCSIT vol. XX (2012), (2012) Singapore: IACSIT Press.

Ramírez-Revilla, S. A., Guzmán, J. J. M., Cipriano, K. N., & Braga, S. L. (2022). Influence of dust deposition, wind and rain on photovoltaic panels efficiency in Arequipa – Peru. *International Journal of Sustainable Energy, 41*, 1369–1382.

Schindelin, J., Arganda-Carreras, I., Frise, E., Kaynig, V., Longair, M., Pietzsch, T., Preibisch, S., Rueden, C., Saalfeld, S., Schmid, B., Tinevez, J.-Y., White, D. J., Hartenstein, V., Eliceiri, K., Tomancak, P., & Cardona, A. (2012). Fiji: An open-source platform for biological-image analysis. *Nature Methods, 9*, 676–682.

Shao, Y., & Lu, H. (2000). A simple expression for wind erosion threshold friction velocity. *Journal of Geophysical Research, 105*, 22437–22443.

Smestad, G. P., Germer, T. A., Alrashidi, H., Fernández, E. F., Dey, S., Brahma, H., Sarmah, N., Ghosh, A., Sellami, N., Hassan, I. A. I., Desouky, M., Kasry, A., Pesala, B., Sundaram, S., Almonacid, F., Reddy, K. S., Mallick, T. K., & Micheli, L. (2020). Modelling photovoltaic soiling losses through optical characterization. *Scientific Reports, 10*, 58.

Solyali, D., & Mollaei, A. (2025). A simulation model based on experimental data to determine the optical tilt angle for a fixed photovoltaic panel. *Archives of Advanced Engineering Science, 3*, 11–21.

Stankov, B., Terziev, A., Vassilev, M., & Ivanov, M. (2024). Influence of wind and rainfall on the performance of a photovoltaic module in a dusty environment. *Energies, 17*, 3394.

Styszko, K., Jaszczur, M., Teneta, J., Hassan, Q., Burzyńska, P., Marcinek, E., Łopian, N., & Samek, L. (2019). An analysis of the dust deposition on solar photovoltaic modules. *Environmental Science and Pollution Research International, 26*, 8393–8401.

Syafiq, A., Balakrishnan, V., Ali, M. S., Dhoble, S. J., Rahim, N. A., Omar, A., & Bakar, A. H. A. (2022). Application of transparent self-cleaning coating for photovoltaic panel: A review. *Current Opinion in Chemical Engineering, 36*, 100801.

Yao, W., Kong, X., Xu, A., Xu, P., Wang, Y., & Gao, W. (2023). New models for the influence of rainwater on the performance of photovoltaic modules under different rainfall conditions. *Renewable & Sustainable Energy Reviews, 173*, 113119.

Zhao, W., Lu., Y., Zhou, Q., & Yan, W. (2021). Collision-adhesion mechanism of particles and dust deposition simulation on solar PV models. *Renewable Energy, 176*, 169–182.

Zorn, E., & Walter, T. R. (2016). Influence of volcanic tephra on photovoltaic (PV)-modules: An experimental study with application to the 2010 Eyjafjallajökull eruption, Iceland. *Journal of Applied Volcanology, 5*, 2.

Publisher's Note